


Article

Model for Predicting Horizontal Well Transient Productivity in the Bottom-Water Reservoir with Finite Water Bodies

Xiaofei Jia ^{1,2}, Zhaobo Sun ³, Guanglun Lei ^{1,4} and Chuanjin Yao ^{1,4,*} ¹ School of Petroleum Engineering, China University of Petroleum (East China), Qingdao 266580, China² China National Offshore Oil Corporation, China Limited, Tianjin Branch, Tianjin 300459, China³ China National Offshore Oil Corporation, International Limited, Beijing 100029, China⁴ Key Laboratory of Unconventional Oil & Gas Development (China University of Petroleum (East China)), Ministry of Education, Qingdao 266580, China

* Correspondence: cy375@upc.edu.cn

Abstract: To better understand the horizontal well transient productivity in the bottom-water reservoir with finite water bodies, the horizontal well transient productivity model for the bottom-water reservoir with finite water-body multiple was developed using Green's function and potential superposition method. Laplace transforms, Fourier transforms, superposition of point source, and Duhamel principle were used to obtain the transient productivity of the horizontal well, and the transient productivity of the horizontal well in real space was obtained by the Stehfest numerical inversion method. The typical pressure response curve and dimensionless productivity curves were plotted. The effects of the water-body multiple, the distance between the horizontal well and oil–water contact, and the skin factor, were analyzed. Six main flowing stages were divided for horizontal wells in the bottom-water reservoir with finite water bodies. When the water body multiples are zero or tend to infinity, the results obtained from the model are consistent with the calculations by the conventional top-bottom closed reservoir model or infinite rigid bottom-water reservoir model, respectively, and the pressure dynamic for the finite water body falls in between both. With the increase in the water body multiples and the decrease in distance between the horizontal well and the oil–water contact, and the horizontal well productivity decreases slowly. With the increase in the skin factor, the initial productivity decreases; moreover, the skin factor has a great influence on the initial productivity of the horizontal well, while the later influence gradually decreases. Accurate horizontal well productivity prediction in the bottom-water reservoir with finite water bodies provides a strong basis for horizontal well deployment, design optimization, and formulation of development policy.

Keywords: finite water bodies; bottom-water reservoir; horizontal well; transient productivity; pressure response



Citation: Jia, X.; Sun, Z.; Lei, G.; Yao, C. Model for Predicting Horizontal Well Transient Productivity in the Bottom-Water Reservoir with Finite Water Bodies. *Energies* **2023**, *16*, 1952. <https://doi.org/10.3390/en16041952>

Academic Editor: Dameng Liu

Received: 23 November 2022

Revised: 12 February 2023

Accepted: 14 February 2023

Published: 16 February 2023



Copyright: © 2023 by the authors. Licensee MDPI, Basel, Switzerland. This article is an open access article distributed under the terms and conditions of the Creative Commons Attribution (CC BY) license (<https://creativecommons.org/licenses/by/4.0/>).

1. Introduction

At present, scholars at home and abroad have conducted a large number of studies on horizontal well production prediction in bottom-water reservoirs, mainly for infinite rigid bottom-water reservoirs [1–37]. However, there are fewer studies on horizontal well production in bottom-water reservoirs with finite water bodies.

Studies of steady-state production from horizontal wells in bottom-water reservoirs date back to the 1980s, and current research is more mature than before. Foreign scholars such as Giger and Kuchuk studied earlier in this field [1,2]. Giger proposed a critical production formula for bottom-water reservoirs in 1986 [1]. Kuchuk et al. derived a production formula for a horizontal well in an infinitely extended bottom-water reservoir in the horizontal direction in 1988 by assuming a constant pressure boundary and a closed boundary in the reservoir and using the cosine transformation method [2]. Following this, many researchers considered the impact of factors such as seepage barriers on the critical production of horizontal wells in bottom-water reservoirs on this basis [3–5]. Domestic

scholar Fan Zifei studied earlier [6,7]. Fan Zifei derived the production equation for a horizontal well in an infinitely extended bottom water-driven reservoir in the horizontal direction in 1993, taking into account the influence of the closed boundary at the top of the reservoir, the constant pressure boundary, the anisotropy of the reservoir, and the horizontal well location on the horizontal well potential distribution in the derivation process. After this, academics such as Cheng Songlin, Dou Hongen, and Chen Yuanqian studied the critical production model for horizontal wells in bottom-water reservoirs using different methods and from different perspectives [8–12]. The steady-state production theory for horizontal wells in bottom-water reservoirs is mainly for infinite rigid water reservoirs and does not apply to the initial production prediction of horizontal wells in bottom-water reservoirs with finite water bodies, nor can it predict the production variation pattern.

Studies of transient productivity from horizontal wells in bottom-water reservoirs date back to the late 1980s. For foreign research, Dikken was the first to use the wellbore friction coefficient formula in conventional pipe flow to calculate horizontal wellbore friction losses in 1989 [13], assuming a constant fluid production index per unit wellbore length in horizontal wells, linking reservoir seepage to wellbore flow through the mass conservation equation in the wellbore, and establishing a transient productivity model. After this, many scholars introduced acceleration pressure drop and proposed a wellbore pressure drop calculation model. They comprehensively considered the flow characteristics in the horizontal wellbore and regarded the friction coefficient as a variable to establish a horizontal well segmental coupling model [14–21]. Domestic scholars have also studied the transient productivity of horizontal wells in bottom-water reservoirs in greater depth. The research methods include mainly analysis methods, physical simulations, and numerical simulations [22–37]. Liu Xiangping, Xiong Jun, Zheng Qiang, Zhou Daiyu, and other researchers established a coupled model of seepage flow and wellbore pressure drop in unsteady reservoirs and carried out analytical calculations of transient productivity in horizontal wells in bottom-water reservoirs and analyzed the variation patterns of indicators such as production along the wellbore and wellhead. Green's function, source function, Laplace transform, and orthogonal transform were used, and conditions including a segmented bare hole in horizontal wells, shot hole completion, variable density shot hole, and reservoir inhomogeneity were considered [22–28]. Wang Jialu and Liu Xinying studied the variation law of production and bottom-water ridge entry of horizontal wells in bottom-water reservoirs through indoor physical simulation experiments [29–31]. Cui Chuanzhi, Jiang Hanqiao, and other scholars studied the characteristic laws of horizontal well production and water flooding in bottom-water reservoirs using reservoir numerical simulation [32–37]. These studies have all been conducted on infinite rigid water reservoirs. They have not considered the effect of finite water-body multiples on horizontal well production and do not apply to horizontal well production prediction in the bottom-water reservoir with finite water bodies.

This paper establishes an unstable production model for horizontal wells in bottom-water reservoirs with finite water bodies with respect to the characteristics of bottom-water reservoirs with finite water bodies, makes dimensionless productivity curves and analyzes the factors influencing production, which can provide a decision basis for the horizontal well deployment, design optimization, and development technology policy formulation in bottom-water reservoirs with finite water bodies.

2. Model Building

2.1. Physical Model

A schematic diagram of the horizontal well development model for a bottom-water reservoir with finite water bodies is shown in Figure 1. The reservoir is laterally infinite. Additionally, the reservoir is vertically divided into the following two parts: the upper part is the unutilized oil layer, and the lower part is the water layer. The upper and lower layers have different pore permeability characteristics.

The model assumes that the following: (i) the top of the thick formation is closed, the thickness of the upper unutilized oil layer is h_1 , the horizontal permeability is k_{h1} , the vertical permeability is k_{v1} , the integrated compression factor is C_{t1} , the porosity is φ_1 , and the crude oil viscosity is μ_o ; (ii) the bottom of the thick oil layer is closed, the thickness of the lower water layer sand body is h_2 , i.e., the water-body multiple is $n = h_2/h_1$, the horizontal permeability is k_{h2} , the vertical permeability is k_{v2} , the integrated compression coefficient is C_{t2} , the porosity is φ_2 , and the viscosity of the formation water is μ_w ; (iii) The fluid is single-phase and slightly compressible. The gravity and capillary forces of the model are neglected. The percolation satisfies Darcy’s law; (iv) Horizontal well length is L_h , and the distance of the horizontal well from the oil–water contact is z_w . The model is produced at a production rate of q with an infinite inflow capacity.

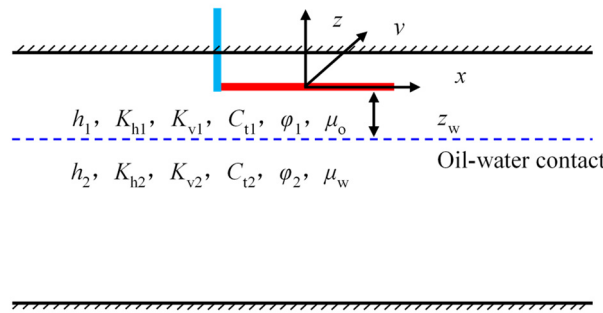


Figure 1. Physical model of a horizontal well in a bottom-water reservoir with finite water bodies.

2.2. Mathematical Modeling and Solving

The dimensionless seepage control equations can be represented as follows:

$$\begin{cases} \frac{\partial^2 p_{D1}}{\partial x_D^2} + \frac{\partial^2 p_{D1}}{\partial y_D^2} + \frac{\partial^2 p_{D1}}{\partial z_D^2} = \frac{\partial p_{D1}}{\partial t_D} \\ \frac{\partial^2 p_{D2}}{\partial x_D^2} + \frac{\partial^2 p_{D2}}{\partial y_D^2} + \lambda \frac{\partial^2 p_{D2}}{\partial z_D^2} = \frac{1}{\eta} \frac{\partial p_{D2}}{\partial t_D} \end{cases} \quad (1)$$

The initial condition can be represented as follows:

$$p_{D1}(x, y, z, t = 0) = p_{D2}(x, y, z, t = 0) = 0 \quad (2)$$

The external boundary condition can be represented as follows:

$$p_{D1}(r \rightarrow \infty, z, t) = p_{D2}(r \rightarrow \infty, z, t) = 0 \quad (3)$$

The top-bottom closed boundary condition can be represented as follows:

$$\frac{\partial p_{D1}(x, y, h_1 - z_w, t)}{\partial z_D} = \frac{\partial p_{D2}(x, y, -h_2 - z_w, t)}{\partial z_D} = 0 \quad (4)$$

The coupling conditions at the oil–water contact can be represented as follows:

$$\begin{cases} p_{D1}(x, y, -z_w, t) = p_{D2}(x, y, -z_w, t) \\ \frac{K_{v1}}{\mu_o} \frac{\partial p_{D1}(x, y, -z_w, t)}{\partial z_D} = \frac{K_{v2}}{\mu_w} \frac{\partial p_{D2}(x, y, -z_w, t)}{\partial z_D} \end{cases} \quad (5)$$

Define the dimensionless variable as $p_{D1} = \frac{\sqrt{K_{h1}K_{v1}}L_h(p_i-p_1)}{1.842 \times 10^{-2}q\mu_o}$; $p_{D2} = \frac{\sqrt{K_{h1}K_{v1}}L_h(p_i-p_2)}{1.842 \times 10^{-2}q\mu_w}$;
 $t_D = \frac{3.6K_{h1}t}{\varphi_1\mu_o C_{t1}}$; $\eta = \left(\frac{K_{h2}}{\varphi_2\mu_w C_{t2}}\right) / \left(\frac{K_{h1}}{\varphi_1\mu_o C_{t1}}\right)$; $h_{D1} = \frac{2h_1}{L_h} \sqrt{\frac{K_{h1}}{K_{v1}}}$; $h_{D2} = \frac{2h_2}{L_h} \sqrt{\frac{K_{h2}}{K_{v2}}}$; $x_D = \frac{2x}{L_h} \sqrt{\frac{K_{h1}}{K_{v1}}}$;
 $y_D = \frac{2y}{L_h} \sqrt{\frac{K_{h1}}{K_{v1}}}$; $z_D = \frac{2z}{L_h} \sqrt{\frac{K_{h1}}{K_{v1}}}$; $z_{wD} = \frac{2z_w}{L_h} \sqrt{\frac{K_{h1}}{K_{v1}}}$; $L_D = \frac{L_h}{2h_1} \sqrt{\frac{K_{v1}}{K_{h1}}}$; $C_D = \frac{2C}{\pi\varphi_1 C_{t1} h_1 L_h}$.

A Laplace transform on t_D for both ends of Equation (1) yields, and it is obtained that

$$\begin{cases} \frac{\partial^2 \bar{p}_{D1}}{\partial x_D^2} + \frac{\partial^2 \bar{p}_{D1}}{\partial y_D^2} + \frac{\partial^2 \bar{p}_{D1}}{\partial z_D^2} = s \bar{p}_{D1} \\ \frac{\partial^2 \bar{p}_{D2}}{\partial x_D^2} + \frac{\partial^2 \bar{p}_{D2}}{\partial y_D^2} + \lambda \frac{\partial^2 \bar{p}_{D2}}{\partial z_D^2} = \frac{s}{\eta} \bar{p}_{D2} \end{cases} \tag{6}$$

Using the Green’s function method, Equation (6) is transformed into the following:

$$\begin{cases} \left(\frac{\partial^2}{\partial x_D^2} + \frac{\partial^2}{\partial y_D^2} + \frac{\partial^2}{\partial z_D^2} - s \right) \bar{G}_1(s, r, r') = -\delta(r - r') \\ \left(\frac{\partial^2}{\partial x_D^2} + \frac{\partial^2}{\partial y_D^2} + \lambda \frac{\partial^2}{\partial z_D^2} - \frac{s}{\eta} \right) \bar{G}_2(s, r, r') = 0 \end{cases} \tag{7}$$

A Fourier cosine transformation of x, y in Equation (7) yields, and it is obtained that

$$\begin{cases} \left(\frac{\partial^2}{\partial z_D^2} - v_1^2 \right) \hat{\hat{G}}_1 = -\delta(r - r') \\ \left(\frac{\partial^2}{\partial z_D^2} - v_2^2 \right) \hat{\hat{G}}_2 = 0 \end{cases} \tag{8}$$

where,

$$v_i^2 = \frac{1}{\lambda_i} \left(\alpha^2 + \beta^2 + \frac{s}{\kappa_i} \right) \tag{9}$$

where α and β are the variables of x , and y in Fourier space, respectively.

The general solution of the above equations can be represented as follows:

$$\begin{cases} \hat{\hat{G}}_1(s, \alpha, \beta, z) = \frac{\pi}{4v_1} e^{-v_1|z-z'|} + A_1 e^{v_1 z} + B_1 e^{-v_1 z} \\ \hat{\hat{G}}_2(s, \alpha, \beta, z) = A_2 e^{v_2 z} + B_2 e^{-v_2 z} \end{cases} \tag{10}$$

Using the laws of transmission and reflection as pressure propagates through different reservoir media, according to Refs. [2,38], it is obtained that

$$\begin{aligned} \hat{\hat{G}}_1(s, \alpha, \beta, r_w) = \frac{\pi}{4v_1} \frac{1}{1 - \Phi_{u1} \Phi_{d1} e^{-2v_1 h_1}} \times & \left[(1 + \Phi_{d1} e^{-2v_1 z_w}) \Phi_{u1} e^{-2v_1 (h_1 - z_w)} \right. \\ & \left. + (1 + \Phi_{u1} e^{-2v_1 (h_1 - z_w)}) \Phi_{d1} e^{-2v_1 z_w} \right] \end{aligned} \tag{11}$$

where u and d are the upward and downward reflection coefficients, respectively.

Combining with the coupling conditions at the oil–water contact, it is obtained that

$$\Phi_{u1} = 1 \tag{12}$$

$$\Phi_{d1} = e^{-2v_2 h_2} \tag{13}$$

Bring Equations (12) and (13) into Equation (11) and simplify to obtain the Green’s point source function within the oil layer in Fourier space.

$$\hat{\hat{G}}_1(s, \alpha, \beta, z, z') = \frac{\pi}{4v_1} e^{-v_1|z-z'|} + \frac{\pi}{4v_1} \frac{\left[e^{-(v_1 z + v_2 h_2)} + e^{-(v_1 h_1 - v_1 z)} \right]^2}{1 - e^{-2(v_1 h_1 + v_2 h_2)}} \tag{14}$$

The pressure response solution for a horizontal well in Laplace space is obtained by taking two Fourier cosine inversions of the above equation and integrating them along the horizontal wellbore.

$$\bar{p}_{wD}(s, r_{wD}) = \frac{2}{s} \left[\bar{p}_{wuD}(s, r_{wD}) + \frac{4}{\pi^2} \int_0^\infty d\alpha \frac{\sin^2 \alpha}{\alpha^2} \int_0^\infty d\beta \hat{G}_{h1}(s, \alpha, \beta, r_{wD}) \right] \tag{15}$$

where,

$$\bar{p}_{wuD}(s, r_{wD}) = \frac{1}{2} \left[\frac{K_0(r_{wD}\sqrt{s})}{r_w\sqrt{s}K_0(r_{wD}\sqrt{s})} - \frac{1 - e^{-2\sqrt{s}}}{2\sqrt{s}} - E_1(2\sqrt{s}) \right] \tag{16}$$

$$\hat{G}_{h1}(s, \alpha, \beta, r_{wD}) = \frac{\pi}{4v_1} \frac{[e^{-(v_1z_{wD}+v_2h_{D2})} + e^{-(v_1h_{D1}-v_1z_{wD})}]^2}{1 - e^{-2(v_1h_{D1}+v_2h_{D2})}} \tag{17}$$

Considering the effect of wellbore storage and skin effect, according to Duhamel’s principle, it is obtained that

$$\bar{p}_{wD} = \frac{s\bar{p}_{wD} + S}{s + s^2C_D(s\bar{p}_{wD} + S)} \tag{18}$$

Equation (18) is transformed to obtain the following:

$$\bar{q}_{wD} = \frac{1}{s^2\bar{p}_{wD}} \tag{19}$$

By numerically inverting the above equation using the Stehfest method, a horizontal well pressure response curve for a bottom-water reservoir with finite water bodies can be plotted, and the transient productivity of a horizontal well can also be calculated [39].

3. Typical Curve Analysis

3.1. Model Verification

As shown in Figure 2, the type curves of pressure obtained by the Saphir numerical solution and the analytical solution proposed in this paper are anastomotic when water-body multiples are set to 50. The curves show the common characteristics. The pressure derivative curve is a 0.5 horizontal line at the early vertical radial flow stage, the slope of the pressure derivative curve is -0.5 at the hemispherical flow stage, while it is an $L_D/51$ horizontal line at the late system pseudo-radial flow stage. Thus, the model and solution in the paper are reliable.

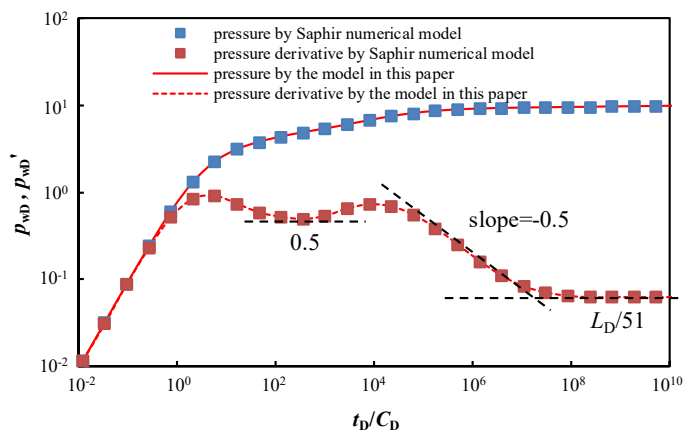


Figure 2. Comparison between the numerical solution and the analytical solution ($n = 50$).

3.2. Typical Curve

The newly established model can solve the pressure in constant production. Therefore, the parameters were selected as the dimensionless wellbore storage factor $C_D = 0.00001$, the skin factor $S = 0.1$, the horizontal well dimensionless length $L_D = 3.2$, and the dimensionless distance between the horizontal well and the oil–water contact $z_{wD} = 0.5$. The pressure and pressure derivative of a horizontal well in bottom-water reservoirs with different water-body multiples ($n = 5, 20$, and 100) are calculated by using the model. The typical curves of pressure and pressure derivative for horizontal wells in bottom-water reservoirs with limited water-body multiples are drawn (Figure 3). The results calculated for the conventional top-bottom closed reservoir model and the infinite rigid bottom-water reservoir model (top closed, constant pressure at the oil–water contact) are plotted on the same plate for comparison and analysis of their flow regimes (Figure 3).

From the three sets of double logarithmic curves for $n = 5, 20$, and 100 in Figure 3, it can be seen that there are six main flow regimes in the seepage process of horizontal wells in bottom water reservoirs with finite water bodies. (I) Early wellbore storage effect stage: the pressure and pressure derivative curves in this stage show a straight line with a slope of 1; (II) transition section between the wellbore storage effect stage and the early vertical radial flow stages: the larger the skin factor, the higher the hump; (III) early vertical radial flow stage: fluid flows in the vertical plane towards the wellbore (Figure 4a), and the pressure derivative curve in this stage shows a horizontal line with a value of 0.5; (IV) transition section between the early vertical radial flow phase and the hemispherical flow stage: pressure waves gradually propagate from the vicinity of the horizontal wellbore towards the top closed boundary; (V) hemispherical flow stage: the pressure wave propagates continuously in the direction of the bottom, and the fluid flows in a hemispherical flow in the vertical direction towards the horizontal well before propagating to the bottom closed boundary (Figure 4b). The hemispherical flow stage lasts longer as the water-body multiple increases, and the pressure derivative curve gradually shows a straight line with a slope of -0.5 ; (VI) late system pseudo-radial flow stage: after the pressure wave propagates to the bottom closed boundary, the pressure propagates in the plane in an (elliptical) circle to the distance, and the reservoir fluid flows in the form of pseudo-radial flow to the horizontal well (Figure 4c). The pressure derivative curve in this stage presents a horizontal line with the value of $L_D/(n + 1)$, which is a unique characteristic of the horizontal well of a bottom-water reservoir with finite water bodies. The size of the water-body multiple in the bottom-water reservoirs with finite water bodies can be determined by the ratio of the pressure derivative value of late system pseudo-radial flow to the pressure derivative value of early vertical radial flow, whose value is $2L_D/(n + 1)$.

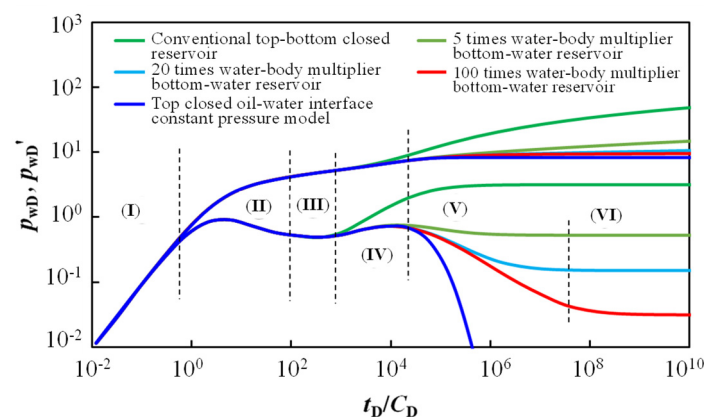


Figure 3. Typical pressure curves of a horizontal well in a bottom-water reservoir with a finite body of water.

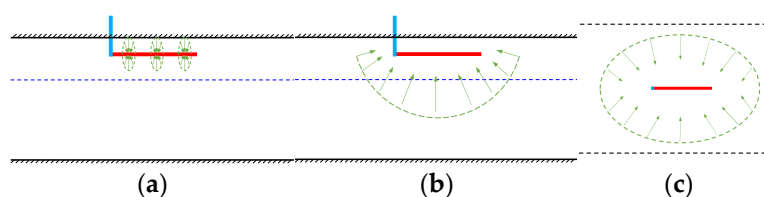


Figure 4. Typical flow patterns of horizontal wells in bottom water reservoir with finite water bodies. (a) Early vertical radial flow stage; (b) hemispherical flow stage; (c) late system pseudo radial flow stage.

As can be seen from the double logarithmic curves of the top-bottom closed common reservoir in Figure 3, there are five main flow regimes in the horizontal well seepage process in top-bottom closed normal reservoirs. The first three stages are consistent with a finite water body bottom-water reservoir, and the last two stages are different. This is consistent with the existing research conclusions, which proves the rationality of the results in this paper [39]. For conventional top-bottom closed reservoirs, the fourth stage (IV) is the linear flow stage. This stage begins after the fluid flows in the vertical plane towards the wellbore and reaches the top-bottom boundary, which is a linear flow of fluid between the upper and lower reservoir boundaries, with the pressure derivative curve showing a straight-line segment with a slope of 0.5. The fifth stage (V) is the late pseudo-radial flow stage: the pressure wave has propagated farther away from the wellbore and approximates a straight well in production relative to the entire seepage range, with fluids converging on the wellbore from all directions to form a radial flow, and the pressure derivative curve is horizontal at this stage.

As can be seen from the double logarithmic curve of the top-closed, oil–water contact constant pressure reservoir in Figure 3, there are five main flow regimes in the seepage process of a horizontal well in an infinite rigid bottom-water reservoir. The first four stages are consistent with a finite water body bottom-water reservoir; the fifth stage is different. For top-closed, constant-pressure reservoirs at the oil–water contact, the fifth stage (V) is the steady flow stage. After the pressure wave propagates to the bottom constant pressure boundary, the flow pressure at the bottom of the horizontal well gradually stabilizes, the pressure at various points in the reservoir also stabilizes, the pressure curve tends to a horizontal line, and the pressure derivative curve falls rapidly to zero.

Comparing the three types of double logarithmic curves in Figure 3 and the above analysis, it can be seen that, unlike the conventional top-bottom closed reservoir and the infinite rigid bottom-water reservoir horizontal well seepage process, the influence of finite water bodies on the flow characteristics of horizontal wells mainly occurs during and after the propagation of pressure waves to the bottom boundary, where the double logarithmic curves appear significantly different. As the number of water-body multiple increases, the pressure curve and pressure derivative curve of horizontal wells in the bottom-water reservoir with finite water bodies increasingly deviate from the pressure curve and pressure derivative curve of horizontal wells in conventional top-bottom closed reservoirs and increasingly converge to the pressure curve and pressure derivative curve of horizontal wells in infinitely large rigid water bodies. The pressure and pressure derivatives of horizontal wells in bottom-water reservoirs with finite water bodies are between those calculated by the conventional top-bottom closed reservoir model and the infinite rigid bottom-water reservoir model, in line with objective laws.

4. Analysis of Factors Influencing Productivity

4.1. Water-Body Multiplier

The parameters were selected as the dimensionless wellbore storage factor $C_D = 0.00001$, the skin factor $S = 0.1$, the horizontal well dimensionless length $L_D = 3.2$, and the dimensionless distance between the horizontal well and the oil–water contact $z_{wD} = 0.5$. The effect of different water-body multiples ($n = 0, 5, 10, 20$, and 50) on the production of

horizontal wells was calculated using the model, and the results are shown in Figure 5. It can be seen that, (i) at the early stage of horizontal well production, horizontal well dimensionless production decreases with the increase in dimensionless time. The production curves of different water-body multiples overlap, showing no effect of water-body multiples on production. The duration of this stage is relatively short. At this stage, the pressure wave does not propagate to the oil–water contact and is not influenced by the energy of the water body; the process is a depletion development, and the production of the horizontal well declines. (ii) As the time of dimensionless production increases, the dimensionless production of horizontal wells gradually decreases. The overall production curve of horizontal well declines due to a lack of energy for finite water bodies, as opposed to infinite rigid bottom-water reservoirs. (iii) The higher the finite water-body multiple, the smaller the decline in yield. As the water-body multiple increases, the capacity of the water body to replenish energy increases, and the decline in yield decreases and gradually levels off.

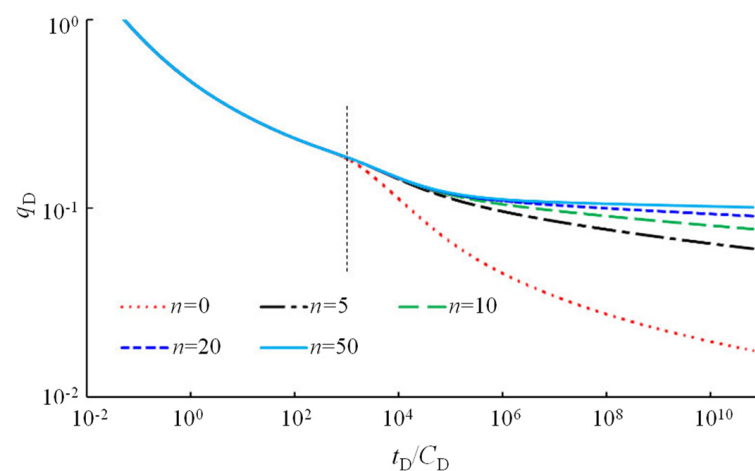


Figure 5. The effect of finite water-body multiple on productivity.

4.2. Distance between Horizontal Well and Oil–Water Contact

The parameters were set as the dimensionless wellbore storage factor $C_D = 0.00001$, the skin factor $S = 0.1$, the horizontal well dimensionless length $L_D = 3.2$, and the finite water-body multiple $n = 50$. The model was used to calculate the effect of different dimensionless distances ($z_{wD} = 0.3, 0.5, 0.7$, and 0.9) between the horizontal well and the oil–water contact on the production of the horizontal well. The results of which are shown in Figure 6. It can be seen that, (i) at the beginning of horizontal well production, horizontal well dimensionless production decreases with the increase in the dimensionless time. The production curves at different distances from the horizontal well and oil–water contact overlap. At this stage, the pressure wave does not propagate to the oil–water contact, and the horizontal well is a depletion development with declining production. (ii) As the time of dimensionless production increases, the dimensionless production of horizontal wells gradually decreases. Unlike infinite rigid bottom-water reservoirs, the overall performance is characterized by a lack of energy in finite water bodies and a decline in horizontal well production. (iii) The smaller the distance between the horizontal well and the oil–water contact, the smaller the rate of production declines. The closer the horizontal well is to the oil–water contact, the greater the pressure gradient acting on the horizontal well, the greater the energy supply, and the smaller the production decline.

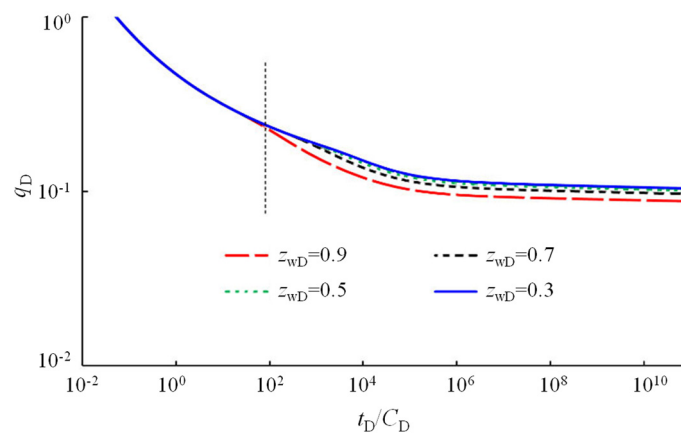


Figure 6. Relationship between the distance of a horizontal well from the oil–water contact and productivity.

4.3. Skin Factor

The parameters selected were the dimensionless wellbore storage factor $C_D = 0.00001$, the dimensionless distance between the horizontal well and the oil–water contact $z_{wD} = 0.5$, the horizontal well dimensionless length $L_D = 3.2$, and the finite water-body multiple $n = 50$. The model was used to calculate the effect of the skin factor ($S = 0.5, 2.5, \text{ and } 5$) on the production of horizontal wells, and the results are shown in Figure 7. It can be seen that, (i) the dimensionless production of horizontal wells gradually decreases as the dimensionless production time increases. Unlike infinite rigid bottom-water reservoirs, the overall performance is characterized by a lack of energy in finite water bodies and a decline in horizontal well production. (ii) The larger the skin factor, the lower the initial production of the horizontal well. The larger the skin factor, the greater the seepage resistance in the near-well zone, the greater the additional pressure drop, the smaller the pressure gradient acting on the horizontal well, and the lower the horizontal well production. (iii) The skin factor affects the whole process of transient productivity from horizontal wells in bottom-water reservoirs with limited water bodies, but the skin effect has a large impact on production in the early stages of production and becomes less influential in the later stages. This is because the mechanical skin mainly acts in the near-well zone, affecting the seepage capacity of the near-well area. The pressure relief of the near-well zone mainly appears at the early stage of horizontal well production, so it has a more significant impact on early production; with the extension of production time, the impact of the skin on production gradually decreases after the pressure wave propagates to the far-well zone.

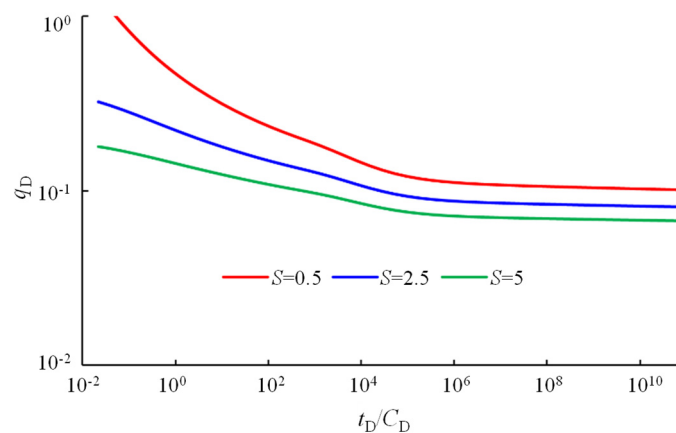


Figure 7. Relationship between skin factor and productivity.

4.4. Field Application

Well A1 is a horizontal well in the LD oilfield in Bohai Bay. The water-body multiple is 18, the total length of the horizontal section of the horizontal well is 456 m, the well radius is 0.12 m, the formation thickness is 8 m, the horizontal well is 6 m from the oil–water contact, the porosity is 32%, the permeability is 1500 mD, the comprehensive compression coefficient is 0.00098, the oil volume coefficient is 1.08, and the formation oil viscosity is 8 mPa·s. The model and method proposed in this paper are used for prediction, resulting in a good agreement between the calculated data and the actual data, as seen in Figure 8.

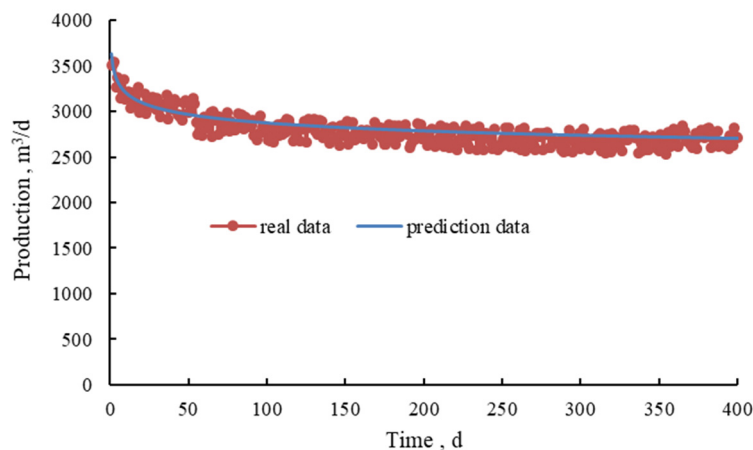


Figure 8. Comparison of model prediction data with real data.

Overall, the model and method proposed in this paper can be used to effectively perform the production analysis of a horizontal well in a bottom-water reservoir with finite water bodies, which broadens the research means of productivity and is more convenient and faster than numerical simulation in the analysis of different parameters.

5. Conclusions

The commonly used horizontal well production model for bottom-water reservoirs treats bottom-water as an infinite rigid body of water and does not consider the effect of the size of the water body. In response to the above problem, a semi-analytical model of the coupled flow between the oil formation and the finite water body was developed using Green's function and potential superposition method. Moreover, the effects of factors including water-body multiples, horizontal well locations, and skin effect on the production of horizontal wells in bottom-water reservoirs with finite water bodies were studied.

Seepage in horizontal wells in bottom-water reservoirs with finite water bodies can be divided into six main flow regimes. As the water-body multiple increases, the hemispherical flow duration is longer, the pseudo-radial flow in the later stage system appears later, and the pressure derivative value is lower. This law can be used for the pressure dynamic analysis of horizontal wells in this type of reservoir.

Production from horizontal wells in bottom-water reservoirs with finite water bodies is influenced by the water-body multiple, horizontal well location, and skin factor. The larger the finite water-body multiple and the smaller the distance between the horizontal well and the oil–water contact, the smaller the decline in production. The larger the skin factor, the lower the initial production of the horizontal well, the greater the early-stage impact, and the smaller the later-stage impact. For reservoirs with a defined water-body multiple, optimizing the distance between the horizontal well and the oil–water contact and improving the drilling process to reduce the surface skin are important ways to increase the production of horizontal wells in bottom-water reservoirs with limited water bodies.

Author Contributions: Conceptualization, X.J.; data curation, X.J., Z.S. and C.Y.; formal analysis, X.J. and G.L.; investigation, X.J., Z.S., G.L. and C.Y.; methodology, X.J.; supervision, G.L. and C.Y.; writing—original draft, X.J.; writing—review and editing, X.J. and C.Y. All authors have read and agreed to the published version of the manuscript.

Funding: This research was funded by National Science and Technology Major Project (grant number 2016ZX05058), CNOOC Science and Technology Major Project (grant number YXKY-2018-TJ-04), and the Fundamental Research Funds for the Central Universities (grant number 20CX06070A).

Institutional Review Board Statement: Not applicable.

Informed Consent Statement: Not applicable.

Data Availability Statement: Not applicable.

Acknowledgments: The results of this study could not have been possible without the efforts of the staff on the research team, and, at the same time, we sincerely thank the editors and reviewers for spending their valuable time reviewing and providing valuable comments.

Conflicts of Interest: The authors declare no conflict of interest.

Nomenclature

p_i	original formation pressure, MPa
t	horizontal well production time, d
h_1	thickness of the upper unutilized oil layer, m
k_{h1}	horizontal permeability of the upper unutilized oil layer, $10^{-3} \mu\text{m}^3$
k_{v1}	vertical permeability of the upper unutilized oil layer, $10^{-3} \mu\text{m}^3$
C_{t1}	integrated compression factor of the upper unutilized oil layer, MPa^{-1}
φ_1	porosity of the upper unutilized oil layer, %
p_1	upper unutilized oil layer pressure, MPa
h_2	thickness of the sand body in the lower water layer, m
K_{h2}	horizontal permeability of the sand body in the lower water layer, $10^{-3} \mu\text{m}^3$
K_{v2}	vertical permeability of the sand body in the lower water layer, $10^{-3} \mu\text{m}^3$
C_{t2}	the combined compression coefficient of the sand body in the lower water layer, MPa^{-1}
φ_2	porosity of the sand body in the lower water layer, %
p_2	pressure of the lower water layer, MPa
μ_w	viscosity of the formation water, $\text{mPa}\cdot\text{s}$
μ_o	crude oil viscosity, $\text{mPa}\cdot\text{s}$
L_h	horizontal well length, m
z_w	the distance between the horizontal well and oil–water contact, m
q	horizontal well production, m^3/d
C	wellbore storage factor, m^3/MPa
p_{D1}	dimensionless pressure of the upper unutilized oil layer, dimensionless
p_{D2}	dimensionless pressure of the lower water layer, dimensionless
t_D	dimensionless production time of the horizontal well, dimensionless
η	conductivity factor, dimensionless
h_{D1}	dimensionless thickness of the upper unutilized oil layer, dimensionless
h_{D2}	the dimensionless thickness of the sand body in the lower water layer, dimensionless
x_D	the dimensionless variable in the x-direction, dimensionless
y_D	the dimensionless variable in the y-direction, dimensionless
z_D	the dimensionless variable in the z-direction, dimensionless
z_{wD}	the dimensionless distance between the horizontal well and the oil–water contact, dimensionless
C_D	the dimensionless wellbore storage factor, dimensionless
S	skin factor, dimensionless

References

1. Giger, F.M. Analytic 2-D models of water cresting before the breakthrough of horizontal wells. In Proceedings of the SPE Annual Technical Conference and Exhibition, New Orleans, LA, USA, 5 October 1986.
2. Kuchuk, F.J.; Goode, P.A.; Wikkeson, D.J.; Thambynayagam, R.K.M. Pressure transient behavior of horizontal wells with and without gas cap or aquifer. *SPE Form. Eval.* **1991**, *6*, 86–94. [[CrossRef](#)]
3. Zhang, P.; Wen, X.H. Existence of flow barriers improves horizontal well production in bottom-water reservoirs. In Proceedings of the SPE Annual Technical Conference and Exhibition, Denver, CO, USA, 21–24 September 2008.
4. Yue, P.; Du, Z.M.; Chen, X.F.; Liang, B.S. The critical rate of horizontal wells in bottom-water reservoirs with an impermeable barrier. *Petrol. Sci.* **2012**, *9*, 223–229. [[CrossRef](#)]
5. Deng, Y.; Lu, Y.N.; Ma, C.; Sun, B.; Luo, C.Y. A method to calculate the critical production of horizontal wells in bottom water reservoir. *Well Test.* **2022**, *31*, 1–5.
6. Fan, Z.F. Study for horizontal well's productivity formula in bottom-water drive reservoir. *Pet. Explor. Dev.* **1993**, *20*, 71–75.
7. Fan, Z.F.; Lin, Z.F. A study of critical rate of a horizontal well in a reservoir with bottom-water drive. *Pet. Explor. Dev.* **1994**, *21*, 65–70.
8. Cheng, L.S.; Lang, Z.X.; Zhang, L.H. Reservoir engineering problem of horizontal wells coning in bottom-water driven reservoir. *J. China Univ. Pet.* **1994**, *18*, 43–47.
9. Dou, H. A new method of predicting the productivity of horizontal well. *Oil Drill. Prod. Technol.* **1996**, *18*, 76–81.
10. Dou, H. Calculation of critical production of horizontal well in bottom water reservoir. *Oil Drill. Prod. Technol.* **1997**, *19*, 70–75.
11. Cui, L.P.; He, S.L. Study on production formula for horizontal wells in reservoir with bottom-water. *J. Oil Gas Technol.* **2009**, *31*, 110–113.
12. Chen, Y.Q. New methods to predict critical production rates in horizontal wells with water and gas coning. *China Offshore Oil Gas* **2010**, *22*, 22–26.
13. Dikken, B.J. Pressure drop in horizontal wells and its effect on production performance. *J. Pet. Technol.* **1990**, *42*, 1426–1433. [[CrossRef](#)]
14. Landman, M.J.; Goldthorpe, W.H. Optimization of perforation distribution for horizontal wells. In Proceedings of the SPE Asia-Pacific Conference, Perth, Australia, 4–7 November 1991.
15. Su, Z.; Gudmundsson, J.S. Pressure drop in perforated pipes experiments and analysis. In Proceedings of the SPE Asia Pacific Oil and Gas Conference, Melbourne, Australia, 7–10 November 1994.
16. Penmatcha, V.R.; Arbabi, S.; Aziz, K. Comprehensive reservoir/wellbore model for horizontal wells. *SPE J.* **1999**, *4*, 224–234. [[CrossRef](#)]
17. Ouyang, L.B.; Huang, B. An Evaluation of well completion impacts on the performance of horizontal and multilateral Wells. In Proceedings of the SPE Annual Technical Conference and Exhibition, Dallas, TX, USA, 9–12 October 2005.
18. Papatzacos, P.; Herring, T.R.; Marthinsen, R.; Skjæveland, S.M. Cone breakthrough time for horizontal wells. *SPE Reserv. Eng.* **1991**, *6*, 311–318. [[CrossRef](#)]
19. Guo, B.Y.; Molinard, J.E.; Lee, R.L. A general solution of gas/water coning problem for horizontal wells. In Proceedings of the European Petroleum Conference, Stavanger, Norway, 24–27 May 1992.
20. Umnuayponwiwat, S.; Ozkan, E. Water and gas coning toward finite-conductivity horizontal wells: Cone Buildup and Breakthrough. In Proceedings of the SPE Rocky Mountain Regional/Low-Permeability Reservoirs Symposium and Exhibition, Denver, CO, USA, 12–15 March 2000.
21. Jiang, Y.; Liu, H.Z.; Wang, D.; Wu, H.J.; Huang, L. Study on bottom water reservoir pressure and flow variation regularity. *Pet. Geol. Eng.* **2018**, *32*, 72–74.
22. Liu, X.P.; Guo, C.Z.; Jiang, Z.X.; Liu, X.; Guo, S.P. The model coupling fluid flow in the reservoir with flow in the horizontal wellbore. *Acta Pet. Sin.* **1999**, *20*, 82–86.
23. Xiong, J. *Study on Productivity of Horizontal Well Completion in Different Completion Modes in Bottom Water Reservoir*; Southwest Petroleum University: Chengdu, China, 2014.
24. Xiong, J.; Xiong, Y.M.; Zhang, L.; Pang, H.; Wang, H.L. Productivity forecast and influence factors analysis of segmentally perforated horizontal well in bottom water reservoir. *Spec. Oil Gas Reserv.* **2014**, *21*, 135–138.
25. Zheng, Q.; Tian, J.; Li, F.; Ding, Z.P.; Peng, G.H.; Zhang, B. Model of waterflooding along horizontal wellbore in heterogeneous reservoir with bottom-water. *Sci. Sin. Technol.* **2014**, *44*, 890–896.
26. Zhou, D.Y.; Jiang, T.W.; Feng, J.L.; Liu, H.P.; Bian, W.J. A simplified approach for determining the reasonable water-free production of horizontal well with bottom water drive reservoir. *Acta Pet. Sin.* **2005**, *26*, 86–89.
27. Zhao, C.S.; Wang, H.; Lv, J.R. The deliverability of horizontal wells of the oil-water fluid in bottom water drive reservoir. *Sci. Technol. Eng.* **2011**, *11*, 4433–4435.
28. Li, X.P. Solution of horizontal well percolation models by orthogonal transformation. *China Offshore Oil Gas* **1995**, *9*, 136–140.
29. Wang, J.L.; Liu, Y.Z.; Jiang, R.Y.; Guan, C.Z. 2-D physical modeling of water coning of horizontal well production in bottom water driving reservoirs. *Pet. Explor. Dev.* **2007**, *34*, 590–593.
30. Liu, X.Y.; Hu, P.; Cheng, L.S. Experimental study of horizontal well with bottom water drive. *Pet. Drill. Tech.* **2011**, *39*, 96–99.
31. Liu, X.Y.; Hu, P. A 3-D visible physical experiment on horizontal wells of heterogeneous reservoirs with bottom water. *Acta Pet. Sin.* **2011**, *32*, 1012–1016.

32. Cui, C.Z.; Zhao, X.Y. Model for predicting horizontal well productivity in the reservoirs with Bottom Water. *J. Oil Gas Technol.* **2007**, *29*, 131–134.
33. Jiang, H.Q.; Li, J.J.; Li, J. Numerical simulation of water flooding law in horizontal wells of reservoirs with bottom water. *J. Southwest Pet. Univ.* **2009**, *31*, 172–176.
34. Wang, J.; Liu, H.Q.; Liu, S.Y.; Gong, R.N. A flooding law in horizontal wells of heterogeneous reservoirs with bottom water. *Acta Pet. Sin.* **2010**, *31*, 970–974.
35. Liu, G.W.; Zhou, D.Y.; Jiang, H.Q.; Wang, T.; Li, J.J. Water-out performance and pattern of horizontal wells for marine sandstone reservoirs in Tarim Basin, NW China. *Pet. Explor. Dev.* **2018**, *45*, 128–135. [[CrossRef](#)]
36. Chen, N.; Liu, H.J.; Wei, K. Research on influence factors and economic limits of horizontal well productivity in bottom water reservoir. *J. Chongqing Univ.* **2019**, *21*, 38–41.
37. Du, D.F.; Wang, Y.Y.; Zhao, Y.W.; Sui, P.S.; Xia, X. A new mathematical model for horizontal wells with variable density perforation completion in bottom water reservoirs. *Petrol. Sci.* **2017**, *14*, 383–394. [[CrossRef](#)]
38. Kuchuk, F.J.; Habashy, T. Pressure behavior of horizontal wells in multilayer reservoirs with crossflow. *SPE Form. Eval.* **1996**, *11*, 55–64. [[CrossRef](#)]
39. Stehfest, H. Numerical inversion of Laplace transforms. *Commun. ACM* **1970**, *13*, 47–49. [[CrossRef](#)]

Disclaimer/Publisher’s Note: The statements, opinions and data contained in all publications are solely those of the individual author(s) and contributor(s) and not of MDPI and/or the editor(s). MDPI and/or the editor(s) disclaim responsibility for any injury to people or property resulting from any ideas, methods, instructions or products referred to in the content.